

**SIMULATION AND EXPERIMENTAL STUDY OF DOUBLE HOLES FILM
COOLING**

MOHD HAZIM FADLI BIN AMINNUDDIN

A project report submitted in
fulfillment of the requirement for the award of the
Degree of Master of Mechanical Engineering



Faculty of Mechanical Engineering and Manufacture
University Tun Hussein Onn Malaysia

MARCH 2017

Dedicated to my beloved parents, family, housemates, and foremost all my friends.

Live to eat or eat to live? You decide.



PTTA UTHM
PERPUSTAKAAN TUNKU TUN AMINAH

ACKNOWLEDGEMENT

In the name of Allah I shall begin.

Through the worst and the best out of me, He kept me going forward to achieve what had been fated in this long journey. I shall not stop to reach out the true meaning for the steps that I have taken from the very beginning.

With all my respect and sincerely gratitude to Dr. Mohammad Kamil Abdullah for every words, wisdom, jokes, idea and everything that he thought me during my whole thesis writing and experiment session. Throughout the year we had, so much constraint we had been going through without a single hesitation in decision making. Such a great supervisor.

Special thanks to my beloved housemate Haswira for everything that we had fought and shared before. For every knowledge and ideas, thank you for such memories.

Thanks to all my fellow friends and also staff at Faculty of Mechanical and Manufacture UTHM for all of the support. The friendship, collegiality and support provided by them will not be forgotten. Good comes from God, flawed comes from my own. God bless all of you. Thank you.

ABSTRACT

In the modern gas turbine, film cooling has been widely used to provide thermal protection for the external surface of the gas turbine blades. Numerous number of geometrical arrangement film cooling have been presented for the past 50 years. The main inspiration of the presented geometrical arrangements film cooling are to minimize the effect of lift off phenomena caused by the formation of the Counter Rotating Vortex Pair (CRVP) which commonly discovered in the Single Cylindrical Hole (SCH) arrangement. In order to reduce the CRVP effects, tremendous efforts from the past researchers have been made including the introduction of the Double Cylindrical Hole (DCH). The present study has made use this DCH along with the employment of several geometrical arrangements including pitch distance (POD), length between holes in streamwise direction (LoD), compound angle and upstream ramp. The evaluation of these parameters involved three different blowing ratios, M and two value of the turbulence intensities, Tu . The diameter of the cooling holes in the present study is 4.75mm which taken based on the previous study. The present study has been divided into two major studies namely experimental study and simulation study. The purpose of the experimental study is to validate the present simulation study which making use of an open end wind tunnel. As the validation process shows a good agreement results, 14 more models have been built and tested using simulation study which the total cases considered are 105. As for the result, all the considered cases of DCH shows improvement in comparison with SCH. Each of the considered geometries and flow parameters have their own effects on the film cooling effectiveness which will be elaborate in details in the further chapter. As conclusion, the simulation is having good agreement with the present experimental study and the previous study which is essential to confirm the reliability of the study. Meanwhile, all DCH shows improvement in term of film cooling effectiveness on each of blowing ratio value.

ABSTRAK

Dalam turbin gas moden, filem penyejukan telah digunakan secara meluas untuk memberi perlindungan haba untuk permukaan luar bilah turbin gas. Banyak susunan filem penyejukan dan geometri telah dikemukakan untuk 50 tahun yang lalu. Inspirasi utama dalam memperkenalkan geometri filem penyejukan adalah untuk mengurangkan kesan kenaikan jet yang disebabkan oleh pembentukan *Counter Rotating Vortex Pair* (CRVP) daripada filem penyejukan silinder tunggal (SCH). Dalam usaha untuk mengurangkan kesan CRVP, banyak usaha dari pengkaji yang terdahulu telah dibuat termasuk pengenalan tentang dua filem penyejukan silinder (DCH). Kajian ini telah menggunakan DCH bersama-sama dengan beberapa susunan dan geometri termasuk jarak melintang (POD), panjang antara lubang dari arah menegak (LoD), sudut kompaun dan tanjak awal sebelum lubang penyejukan. Bagi parameter aliran, tiga nisbah tiupan yang berbeza, M dan dua nilai kadar pergolakan, Tu telah dipertimbangkan. Diameter lubang penyejukan dalam kajian ini adalah 4.75mm yang diambil berdasarkan kajian sebelumnya. Kajian ini telah dibahagikan kepada dua kajian utama; kajian eksperimen dan kajian simulasi. Setelah proses pengesahan menunjukkan hasil yang boleh diterima, 14 model yang berbeza telah dibina dan diuji menggunakan kajian simulasi dan jumlah kes yang dipertimbangkan adalah 105. Untuk hasil kajian, semua kes DCH yang dipertimbangkan telah menunjukkan peningkatan dalam keberkesanan filem penyejukan berbanding dengan kes SCH. Setiap geometri dan parameter aliran mempunyai kesan tersendiri pada keberkesanan filem penyejukan yang akan diterangkan dengan lebih terperinci dalam bab-bab yang selanjutnya. Kesimpulannya, hasil kajian simulasi ini mempunyai hasil yang baik setelah dibandingkan dengan hasil kajian eksperimen ini dan ianya penting dalam pengesahan kebolehpercayaan kajian. Sementara itu, semua DCH menunjukkan peningkatan dari segi filem penyejukan keberkesanan pada setiap meniup nilai nisbah.

CONTENTS

	TITLE	i
	DECLARATION	ii
	ACKNOWLEDGEMENT	iv
	ABSTRACT	v
	ABSTRAK	vi
	CONTENTS	vii
	LIST OF TABLES	ix
	LIST OF FIGURES	x
	LIST OF SYMBOLS AND ABBREVIATIONS	xvii
	LIST OF APPENDICES	xviii
CHAPTER 1	INTRODUCTION	1
	1.1 Introduction	1
	1.2 Background of Study	5
	1.3 Problem Statement	5
	1.4 Importance of Research	6
	1.5 Objectives	6
	1.6 Scope of studies	6
CHAPTER 2	LITERATURE REVIEW	8
	2.1 Introduction	8
	2.2 Film cooling and counter rotating vortex pair concepts	9
	2.3 Previous Research	11
	2.3.1 Early development of cooling holes	11
	2.3.2 Upstream ramp effects	13
	2.3.3 Advanced film cooling	14
	2.3.4 Flow parameter of cooling holes	15
	2.3.4.1 Influence of blowing ratios	15

	2.3.4.2 Influence of turbulence intensity	17
CHAPTER 3	METHODOLOGY	19
	3.1 Introduction	19
	3.2 Flow chart	20
	3.3 Simulation study	22
	3.3.1 Computational domain	22
	3.2.2 Mesh dependency test	23
	3.2.3 Boundary condition and simulation setup	26
	3.2.4 Performances indicator	30
	3.4 Experimental study	32
CHAPTER 4	RESULT AND DISCUSSION	38
	4.1 Introduction	38
	4.2 Mesh dependency test	39
	4.3 CFD results validation	41
	4.4 Effects of turbulence intensities on film cooling effectiveness	45
	4.5 Effects of pitch distance on film cooling effectiveness	53
	4.6 Effects of length between holes (LoD) on film cooling effectiveness	60
	4.7 Effects of compound angle on film cooling effectiveness	67
	4.8 Effect of turbulence intensities on film cooling effectiveness	74
	4.9 Area averaged effectiveness vs total pressure loss coefficient	83
CHAPTER 5	CONCLUSION AND RECOMMENDATION	88
	5.1 Conclusion	88
	5.2 Recommendation for Future Work	89
	REFERENCES	91
	APPENDIX	94

LIST OF TABLES

3.1	Flow parameters details	27
3.2	Single cylindrical hole (SCH) coolant mass flow rate	28
3.3	Double cylindrical hole (DCH) coolant mass flow rate	28
3.4	Details of simulation setup	29
3.5	Parameter and apparatus for experimental measurement	36
4.1	The number of nodes and elements for coarse, medium and fine mesh.	39



LIST OF FIGURES

1.1	Gas-turbine engine layout	2
1.2	T - s diagram and P - v diagram	2
1.3	The cooling air passages inside the blade and the others internal cooling hole embedded in turbine blades	4
1.4	Illustration of the geometrical parameters of the present study	7
2.1	The chart of specific core power of gas turbine	9
2.2	Formation of the CRVP by the single cylindrical cooling hole	10
2.3	Formation of vortices produced by the combined hole	10
2.4	Cylindrical hole, Fan-shaped hole, and Laidback fan-shaped hole details	12
2.5	Example of trenched film cooling hole geometry	12
2.6	Test model schematic diagram	14
2.7	Single cylindrical hole arrangement, fan-shaped laidback hole, and double cylindrical holes	15
2.8	Graph of film cooling effectiveness, η versus streamwise location, x/Ms_0 for varying blowing ratio	16
2.9	Comparison of blowing ratios on film cooling effectiveness, η and streamwise location, x/d	16

	from the experimental result of Ligrani and Lee	
2.10	The vorticity contour produced for $M = 1$ and $M = 2$ at plane y/D versus x/D	17
2.11	Influence of turbulence intensity on centerline of film cooling effectiveness, η at different streamwise location, x/D for $M=0.5$ and $M=1.7$	18
2.12	Film cooling effectiveness at low and high turbulence at plane z/D versus x/D	18
3.1	The flowchart details	20
3.2	The flow of components in ANSYS CFX	22
3.3	Isometric view for SCH and DCH	23
3.4	Sample of computational domain	23
3.5(a)	Upstream ramp dimension details; Rectangular ramp	24
3.5(b)	Upstream ramp dimension details; Triangular ramp	24
3.6	Computational domain meshes	25
3.7	Inflation for DCH mesh at the cooling hole	25
3.8	Details of boundary conditions	26
3.9	Experimental layout	32
3.10	The dimension of the flat plate	35
3.11	The location of infrared thermography camera, valves and flat plate	35
3.12(a)	Valve 1 open and Valve 2 closed	34
3.12(b)	Valve 1 closed and Valve 2 open	34
3.13	Graph of y/δ versus u/U_∞ of the velocity profile comparison	35
3.14	Contoured IR Thermography images imported into the Excel grids	37
4.1	Mesh dependency test	40
4.2	Results of the present experiment of case 2D45 on different blowing ratios	41

4.3	Laterally averaged film cooling effectiveness, $\eta_{lat.avg}$ at different location, x/D comparison at $M = 0.5$	42
4.4	Laterally averaged film cooling effectiveness, $\eta_{lat.avg}$ at different location, x/D comparison at $M = 1.0$	42
4.5	Laterally averaged film cooling effectiveness, $\eta_{lat.avg}$ at different location, x/D comparison at $M = 1.5$	43
4.6	All blowing ratio and turbulence intensities for 2D45 at x/D and z/D plane	45
4.7	Temperature distribution contour at y/D and z/D plane for turbulence intensities cases at blowing ratio, $M = 0.5$	46
4.8	Temperature distribution contour at y/D and z/D plane for turbulence intensities cases at blowing ratio, $M = 1.0$	46
4.9	Temperature distribution contour at y/D and z/D plane for turbulence intensities cases at blowing ratio, $M = 1.5$	47
4.10	Laterally averaged film cooling effectiveness, $\eta_{lat.avg}$ at different location, x/D for turbulence intensities cases at $M = 0.5$	48
4.11	Laterally averaged film cooling effectiveness, $\eta_{lat.avg}$ at different location, x/D for turbulence intensities cases at $M = 1.0$	49
4.12	Laterally averaged film cooling effectiveness, $\eta_{lat.avg}$ at different location, x/D for turbulence intensities cases at $M = 1.5$	49
4.13	Type of the vortices formed	50
4.14	The isosurface of the vortices formed	51
4.15	Vorticity contour plot comparison at y/D and z/D plane for turbulence intensities cases	51

4.16	Film cooling distribution PoD and compound angle cases at $M = 0.5, 1.0$ and 1.5 at x/D and z/D plane	53
4.17	Temperature distribution contour for PoD cases at blowing ratio, $M = 0.5$ at y/D and z/D plane	54
4.18	Temperature distribution contour for PoD cases at blowing ratio, $M = 1.0$ at y/D and z/D plane	54
4.19	Temperature distribution contour for PoD cases at blowing ratio, $M = 1.5$ at y/D and z/D plane	55
4.20	Lateral average film cooling effectiveness, $\eta_{lat.avg}$ at different location, x/D of PoD cases at $M = 0.5$	56
4.21	Lateral average film cooling effectiveness, $\eta_{lat.avg}$ at different location, x/D of PoD cases at $M = 1.0$	57
4.22	Lateral average film cooling effectiveness, $\eta_{lat.avg}$ at different location, x/D of PoD cases at $M = 1.5$	57
4.23	Detachment and reattachment for 4D35 case at $M = 1.5$	58
4.24	Vorticity contour plot for 2D35, 3D35 and 4D35 for all blowing ratios at $x/D = 5$ on y/D and z/D plane	59
4.25	Film cooling effectiveness contour of LoD cases on x/D and z/D plane at $M = 0.5$	60
4.26	Temperature distribution contour for LoD cases at blowing ratio, $M = 0.5$ on y/D and z/D plane	61

4.27	Temperature distribution contour for LoD cases at blowing ratio, $M = 1.0$ on y/D and z/D plane	62
4.28	Temperature distribution contour for LoD cases at blowing ratio, $M = 1.5$ on y/D and z/D plane	62
4.29	Laterally averaged film cooling effectiveness, $\eta_{lat.avg}$ at different location, x/D for LoD cases at $M = 0.5$	64
4.30	Laterally averaged film cooling effectiveness, $\eta_{lat.avg}$ at different location, x/D for LoD cases at $M = 1.0$	64
4.31	Laterally averaged film cooling effectiveness, $\eta_{lat.avg}$ at different location, x/D for LoD cases at $M = 1.5$	65
4.32	Vorticity contour plot comparison for LoD cases on y/D and z/D plane	66
4.33	Film cooling distribution for case 3D35, 3D40 and 3D45 at $M=0.5, 1.0$ and 1.5 on x/D and z/D plane	67
4.34	Temperature distribution contour for compound angle cases at blowing ratio, $M = 0.5$ on y/D and z/D plane	68
4.35	Temperature distribution contour for compound angle cases at blowing ratio, $M = 1.0$ on y/D and z/D plane	68
4.36	Temperature distribution contour for compound angle cases at blowing ratio, $M = 1.5$ on y/D and z/D plane	69
4.37	Laterally averaged film cooling effectiveness, $\eta_{lat.avg}$ at different location, x/D for compound angle cases at $M = 0.5$	71

4.38	Laterally averaged film cooling effectiveness, $\eta_{lat.avg}$ at different location, x/D for compound angle cases at $M = 1.0$	71
4.39	Laterally averaged film cooling effectiveness, $\eta_{lat.avg}$ at different location, x/D for compound angle cases at $M = 1.5$	72
4.40	Vorticity contour plot for 3D35, 3D40 and 3D45 for all blowing ratios at $x/D = 5$ on y/D and z/D plane	73
4.41	Comparison of film cooling effectiveness contour between 2D35 and 2D35 upstream ramp cases.	74
4.42	Backflow velocity vector of case 2D35 Rec Ramp at $M = 1.5$	75
4.43	Temperature distribution contour for upstream ramp cases at blowing ratio, $M = 0.5$ on y/D and z/D plane	76
4.44	Temperature distribution contour for upstream ramp cases at blowing ratio, $M = 1.0$ on y/D and z/D plane	76
4.45	Temperature distribution contour for upstream ramp cases at blowing ratio, $M = 1.5$ on y/D and z/D plane	77
4.46	Laterally averaged film cooling effectiveness for upstream ramp cases $M=0.5$	78
4.47	Laterally averaged film cooling effectiveness for upstream ramp cases $M=1.0$	78
4.48	Laterally averaged film cooling effectiveness for upstream ramp cases $M=1.5$	79
4.49	Velocity profile of upstream ramp cases located at $x/D = -1$ and $z/D = 0$ on blowing ratio 0.5	80

4.50	Velocity profile of upstream ramp cases located at $x/D = 0$ and $z/D = 0$ on blowing ratio 0.5	80
4.51	Velocity profile of upstream ramp cases located at $x/D = 1$ and $z/D = 0$ on blowing ratio 0.5	81
4.52	Vorticity contour plot comparison for upstream ramp cases on y/D and z/D plane at different blowing ratio, M	81
4.53	Area averaged effectiveness for all cases	83
4.54	Total pressure losses graph for all cases	85
4.55	Normalize total pressure loss coefficient vs normalize area averaged effectiveness at $M = 0.5$	86
4.56	Normalize total pressure loss coefficient vs normalize area averaged effectiveness at $M = 1.0$	86
4.57	Normalize total pressure loss coefficient vs normalize area averaged effectiveness at $M = 1.5$	87



LIST OF SYMBOLS AND ABBREVIATIONS

A	-	Area
CRVP	-	Counter Rotating Vortex Pair
D, d	-	Diameter
DCH	-	Double Cooling Holes
DR	-	Density Ratio
LoD	-	Distance between holes in streamwise direction
M	-	Blowing ratio
PoD	-	Pitch distance
RANS	-	Reynolds Averaged Navier Stokes
Re	-	Reynolds number
SCH	-	Single cooling hole
T	-	Temperature
T_{jet}	-	Coolant temperature
T_{∞}	-	Mainstream temperature
T_{aw}	-	Surface temperature
Tu	-	Turbulence intensities
u_{jet}	-	Coolant velocity
u_{∞}	-	Mainstream velocity
\mathcal{E}	-	Dimensionless temperature
θ	-	Inclination angle
η	-	Film cooling effectiveness
α	-	Compound angle
\dot{m}	-	Mass flow rate
ρ	-	Density
ρ_{jet}	-	Coolant density
ρ_{∞}	-	Mainstream density

LIST OF APPENDICES

APPENDIX	TITLE	PAGE
A	Gantt chart	87
B	Cases matrix	88
C	Computational domain	89



PT TA UTHM
PERPUSTAKAAN TUNKU TUN AMINAH

INTRODUCTION

CHAPTER 1

1.1 Introduction

Gas turbine engine are widely used in land based power plant and aircraft making its overall efficiency has been a key research topic in the turbo machinery industry. Gas turbine generates power by the burning of gasoline, oil, or other fuel which produces hot gases that will be expanded while producing work. At the early stage of its introduction, gas turbines have been used mainly in the aviation industry to power the aircraft. The history starts when Frank Whittle patented the first gas turbine which involved a compressor unit with two axial stages, followed by a centrifugal stage, an axial cannular combustor with fuel nozzle and two stages axial turbine in 1930 [1]. On 12 April 1937, Whittle has successfully tested the world's first kerosene-fueled jet engine known as Whittle Unit (W.U).

Nowadays, gas turbine has been widely used as power generating devices. In practice, gas turbines operate in an open cycle and Figure 1.1 shows the major parts of the gas turbine consists of compressor, combustor and turbine. During the operation of gas turbines, the fresh air will first drawn into the compressor to increase the pressure of the air before entering the combustion chamber where the air will be mixed with the fuel and burned at constant pressure. The resulting high-temperature gases will enter the turbine where it will be expanded to atmospheric pressure while generating power through the turbine.

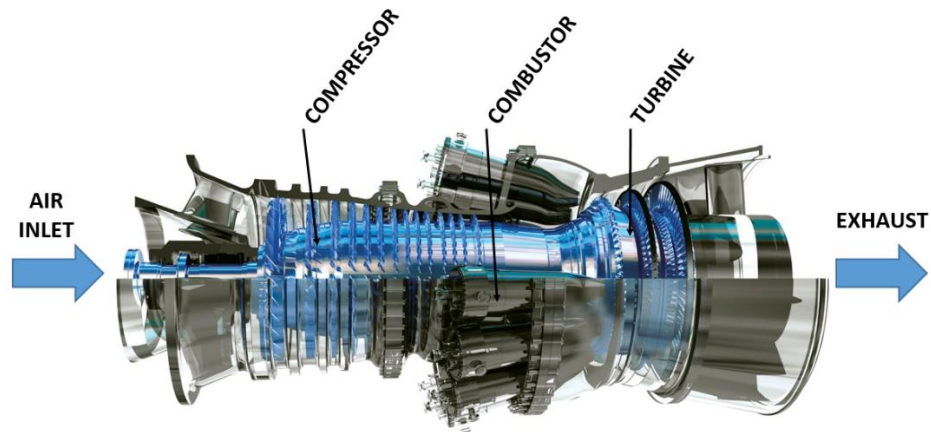


Figure 1.1: Gas-turbine engine layout. (Adapted from [2]).

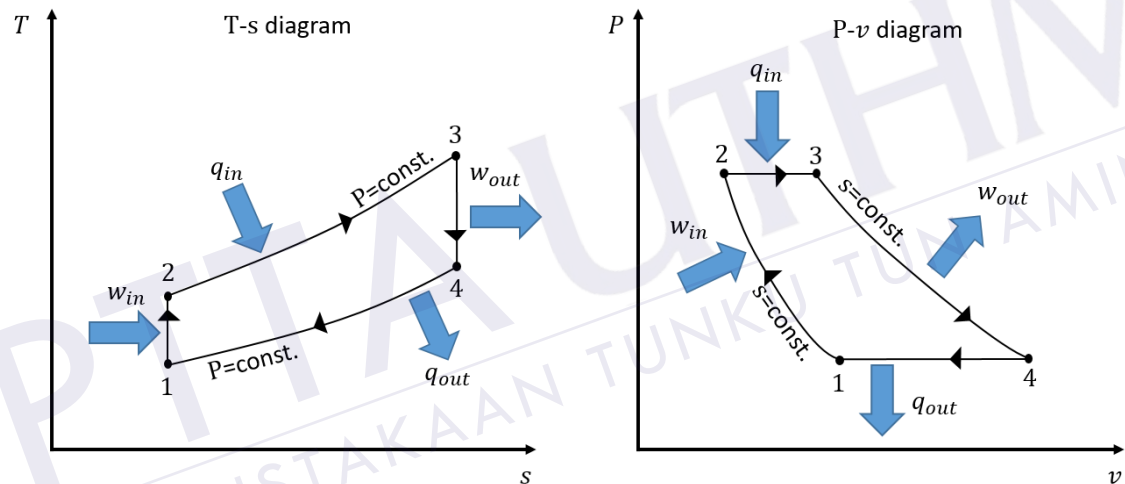


Figure 1.2: T - s diagram and P - v diagram [3].

Figure 1.2 shows the temperature versus entropy, T - s and pressure versus volume, P - v diagrams for gas turbine. Ideally, gas turbine operates in a Brayton's cycle involving four main process [3]. At stage 1-2, fresh ambient air will be drawn in by the compressor and been compressed to a higher temperature and pressure before entering the next stage of 2-3. In this stage, these high pressure air then are sent into a combustion chamber along with the injected fuel, where it is burned at constant pressure, Q_{in} . Meanwhile in stage 3-4, the high temperature gas will flow through the turbine resulting it to expand to the ambient pressure while producing power, W_{out} . Finally at stage 4-1, the exhaust gases leave the turbine with constant pressure heat rejection, Q_{out} . The overall thermal efficiency of the Brayton's cycle as in standard assumption can be given by [3] is

$$\eta_{\text{th,Brayton}} = \frac{w_{\text{nett}}}{q_{\text{in}}} = 1 - \frac{T_4}{T_3} \quad (1.1)$$

Equation 1.1 shows that the efficiency of the gas turbine is proportional towards the turbine inlet temperature (TIT), T_3 , where higher TIT will produce higher cycle efficiency, which has been the approach in development of the modern gas turbine. In comparison with the early stage of gas turbine operation, the modern gas turbines are now operating at temperature exceeding 1800 °C. This high TIT is considered as a significant progress in comparison with the initial TIT of the Whittle's gas turbine which operating at 760 °C [4]. The improvement has been made possible by the progress made in material development and the introduction of thermal cooling system.

In the conventional jet engines, the limiting factor is on the performance of the material used for hot section (e.g.: combustor and turbine). The need for better materials spurred much research in the field of alloys and manufacturing techniques, and resulted in a long list of new materials and methods that make modern gas turbines possible. In the 1940s and 1950s, superalloys and vacuum induction melting which is the new processing methods have been developed and greatly increased the turbine blades temperature capabilities [5]. In modern turbine blade, the material that often used is nickel-based superalloys that incorporate chromium, cobalt and rhenium. Another major improvement to turbine blade material technology was the development of thermal barrier coatings (TBC). As the temperature increases, these TBCs will improve the blade corrosion and oxidation resistance. The first TBCs applied was on 1970s using aluminide coating and in 1980s the coating has been improved into ceramic coating [5]. These coatings improve the turbine blade temperature capabilities nearly 90 °C and also doubling the life of the blades in some cases.

In the later year of gas turbine development, thermal cooling system has help to further improve the overall efficiencies of gas turbines which is embedded in the turbine blades. Thermal cooling systems are divided into two major categories which are the internal cooling and the external cooling [6]. Both of these categories are related towards each other. A cooler air which extracted from the compressor will first be supplied for internal cooling of the blade. This cooled air will went through a flow passage inside the blade while picking up heat during the process. This process also

known as the convection cooling. As the coolant pick-up the heat along the passages, some of the coolant will be released through the film cooling. As for external cooling in the gas turbine, several cooling techniques (impingement cooling, pin fin cooling, rib turbulated cooling and tip cap cooling) have been applied and the present study is focusing on the most common technique, film cooling.

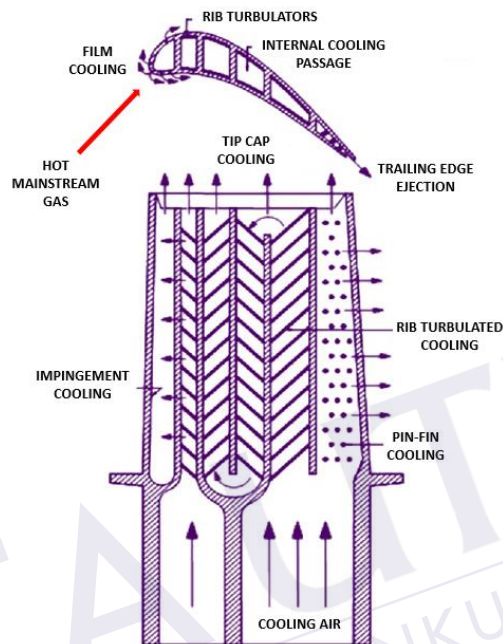


Figure 1.3: The cooling air passages inside the blade and the others internal cooling hole embedded in turbine blades. (Adapted from [7])

1.2 Background of study

The film cooling technique is achieved by allowing the coolant to be injected out from the turbine blade's body through cooling holes. The injected coolant will form a thin cool layer that covering the blade surface. Most of the available film cooling is using a single hole cylindrical or shaped holes. A lot of researches have been done to improve the performance of the film cooling [6]. The film cooling effectiveness produced by a cylindrical hole is exposed to the Counter Rotating Vortex Pair (CRVP) phenomena [7]. This CRVP will affect the film cooling effectiveness, which will further discuss later on in this writing. The present research trend shows a lot of efforts have been made on proposing new cooling hole geometry to reduce the formation of CRVP effect which includes trenched hole and anti-vortex hole. Although the shaped hole known to produce better film cooling effectiveness, single hole is still been used extensively due to its manufacturability. Wright et al. [8] have proposed a new geometry of film cooling known as double cylindrical hole. This geometry utilizes a pair of cylindrical film cooling of approximately the same diameter. Effective utilization of cylindrical hole arrangement will be able to reduce the manufacturing cost associated with shaped hole.

1.3 Problem statements

Previous study of Wright et al. [8] reported that the effects of double film cooling hole arrangement indicates an improvement on the film cooling effectiveness of the cooling hole vicinity areas. However, due to the short distance between the two holes considered; the film cooling effectiveness rapidly decays at further downstream of the cooling hole. By varying the arrangements of double cylindrical holes in terms of streamwise angles and spacing between the holes, better film cooling effectiveness might be produced at further downstream. The present study intended to evaluate the new cooling hole geometrical effects on the performances of the double cylindrical hole arrangement.

1.4 Importance of research

The importance of the present research is to provide extended information on double cylindrical hole film cooling effectiveness at various geometrical and flow parameters. The study will also provides information on the flow field of the double cylindrical hole which could be crucial for future study.

1.5 Objectives

The objectives of the study are:-

- a) To validate the film cooling effectiveness prediction by the experimental.
- b) To predict the film cooling effectiveness of DCH based on the effects of various geometrical and flow parameters
- c) To clarify the performance of upstream ramp in improving the film cooling effectiveness

1.6 Scope of studies

This section will describe on the scope of the study involving the geometrical parameters and flow parameters.

As shown in Figure 1.4, the scope for geometrical parameters of the present study are;

- a) Three compound angle, α are considered; $\alpha = 35^\circ, 40^\circ$ and 45° .
- b) The pitch distance, $PoD = 2D, 3D$ and $4D$.
- c) The distance between holes in streamwise direction, $LoD = 1D, 2D$ and $3D$.
- d) Two types of upstream ramps; Triangular ramp and Rectangular ramp.

Meanwhile, the scope for flow parameters of the present study;

- a) Three blowing ratios, $M = 0.5, 1.0$ and 1.5
- b) Three turbulence intensities, $Tu = 1\%, 5\%$ and 10%
- c) Density ratio, $DR = 1.1$

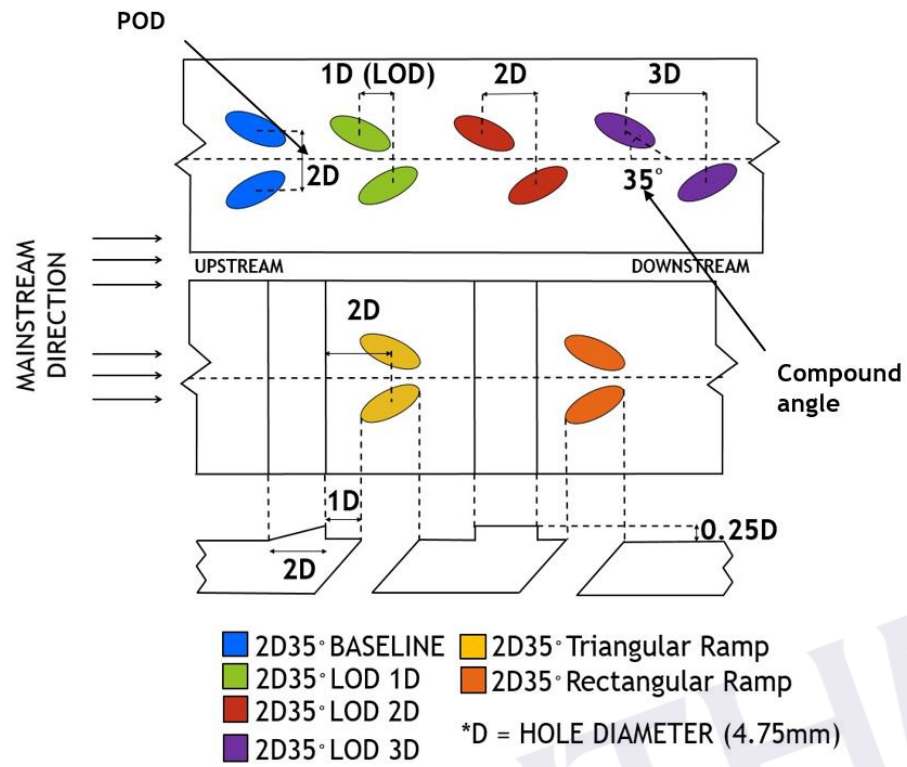


Figure 1.4: Illustration of the geometrical parameters of the present



REFERENCES

- [1] Bill, G. and Patrick, S. (2006) *The Development of Jet And Turbine Aero Engines*. 4th edition. ISBN 0 7509 4477 3, p.124.
- [2] static.progressivemediagroup.com/uploads/imagelibrary/nri/power/news/GE%20Turbine.jpg [accessed on 27 May 2016]
- [3] Çengel, Y. A. and Michael A. B. (2011) *Thermodynamics: An Engineering Approach*. 7th ed. New York: McGraw-Hill, 508-09.
- [4] Bill, G. (2006) *World Encyclopedia of Aero Engines*. 5th edition. Sutton Publishing, p.160.
- [5] Koff, B. L. (2003) *Gas Turbine Technology Overview - A Designer's Perspective*. AIAA/ICAS International Air and Space Symposium and Exposition: The Next 100 Years. AIAA 2003-2722.
- [6] Yahya, S. M. (2010) *Turbines Compressors and Fans*. New Delhi: Tata McGraw-Hill Education, pp. 430–433.
- [7] Han, J. C., Park, J. S., and Lie, C. K. (1984) *Heat Transfer and pressure drop in blade cooling channels with turbulence promoters*. NASA CR-3837.
- [8] Wright, L. M., McClain, S. T., Brown, C. P., and Harmon, W. V. (2013) *Assessment of a Double Hole Film Cooling Geometry Using S-PIV and PSP*. ASME Turbo Expo 2013: Turbine Technical Conference and Exposition, pp. V03BT13A024-V03BT13A024.
- [9] Saunter, M., Clouser, S., and Han, J. C. (1992) *Determination of Surface Heat Transfer and Film Cooling Effectiveness in Unsteady Wake Flow Conditions*. AGARD Conference Proceedings 527, pp. 6-1 to 6-12.
- [10] Han, J. C., Dutta, S. and Ekkad, S. V. (2000) *Gas Turbines Heat Transfer and Cooling Technology*. New York: Taylor and Francis, pp. 646.

- [11] Han, C., and Ren, J. (2012). *Multi-parameter influence on combined-hole film cooling system*. International Journal of Heat and Mass Transfer, 55(15), 4232-4240
- [12] Kwak, J. S., and Han, J. C. (2002). *Heat transfer coefficient and film-cooling effectiveness on a gas turbine blade tip*. ASME Turbo Expo 2002: Power for Land, Sea, and Air, pp. 309-318.
- [13] Haven, B. A., and Kurosaka, M. (1977) *Improved Jet Coverage through Vortex Cancellation*. AIAA Journal. Vol.34, No. 11.
- [14] Eckert, E. R. G., Eriksen, V. L., Goldstein, R. J., and Ramsey, J. W. (1970) *Film cooling following injection through inclined circular tubes*.
- [15] Goldstein, R. J., Eckert, E. R. G., and Burggraf, F. (1974) *Effects of Hole Geometry and Density on Three-Dimensional Film Cooling*. International J. Heat and Mass Transfer. Vol. 17, pp. 595-607.
- [16] Gritsch, M., Schulz A., and Wittig, S. (1998) *Adiabatic Wall Effectiveness Measurements of Film-Cooling Holes with Expanded Exits*. ASME J. Turbomachinery, Vol. 120, pp. 549-556.
- [17] Islami, S. B., Tabrizi, S. A., Jubran, B. A., and Esmaeilzadeh, E. (2010). *Influence of trenced shaped holes on turbine blade leading edge film cooling*. Heat Transfer Engineering, 31(10), 889-906.
- [18] Na, S., and Shih, T. I. (2007). *Increasing adiabatic film-cooling effectiveness by using an upstream ramp*. Journal of heat transfer, 129(4), 464-471.
- [19] Halder, P., and Samad, A. (2012). *Enhancement of Film Cooling Effectiveness Using Upstream Ramp*. ASME 2012 Gas Turbine India Conference, pp. 551-557.
- [20] Barigozzi, G., Franchini, G., and Perdichizzi, A. (2007, January). *The Effect of an Upstream Ramp on Cylindrical and Fan-Shaped Hole Film Cooling: Part I—Aerodynamic Results*. ASME Turbo Expo 2007: Power for Land, Sea, and Air, pp. 105-113.
- [21] Chen, S. P., Chyu, M. K., and Shih, T. I. P. (2011). *Effects of upstream ramp on the performance of film cooling*. International Journal of Thermal Sciences, 50(6), 1085-1094.
- [22] Dhungel, S., Phillips, A., Ekkad, S.V., and Heidmann, J.D. (2007) *Experimental Investigation of a Novel Anti-Vortex Film Cooling Hole Design*. ASME Paper GT2007–27419.

- [23] Heidmann, J. D. (2008, January). *A numerical study of anti-vortex film cooling designs at high blowing ratio*. ASME Turbo Expo 2008: Power for Land, Sea, and Air, pp. 789-799.
- [24] Schulz, S., Maier, S., and Bons, J. P. (2012, June). *An experimental investigation of an Anti-Vortex Film Cooling Geometry Under Low and High Turbulence Conditions*. ASME Turbo Expo 2012: Turbine Technical Conference and Exposition, pp. 1581-1593.
- [25] Baldauf, S., Schulz, A., and Wittig, S. (2001). *High-resolution measurements of local effectiveness from discrete hole film cooling*. Journal of Turbomachinery, 123(4), 758-765.
- [26] Ligrani, P. M., and Lee, J. S. (1996). *Film cooling from a single row of compound angle holes at high blowing ratios*. International Journal of Rotating Machinery, 2(4), 259-267.
- [27] Kadotani, K., and Goldstein, R. J. (1979). *On The Nature of Jets Entering A Turbulent Flow: Part A—Jet–Mainstream Interaction*. Journal of Engineering for Gas Turbines and Power, 101(3), 459-465.
- [28] Launder, B. E., and York, J. (1974). *Discrete-hole cooling in the presence of free stream turbulence and strong favourable pressure gradient*. International Journal of Heat and Mass Transfer, 17(11), 1403-1409.
- [29] Bons, J. P., MacArthur, C. D., and Rivir, R. B. (1996). *The effect of high free-stream turbulence on film cooling effectiveness*. Journal of Turbomachinery, 118(4), 814-825.
- [30] Al-Hamadi, A. K., Jubran, B. A., and Theodoridis, G. (1998). *Turbulence intensity effects on film cooling and heat transfer from compound angle holes with particular application to gas turbine blades*. Energy conversion and management, 39(14), 1449-1457.
- [31] Amer, A. A., Jubran, B. A., and Hamdan, M. A. (1992). *Comparison of different two-equation turbulence models for prediction of film cooling from two rows of holes*. Numerical Heat Transfer, 21(2), 143-162.
- [32] Markatos, N. C. (1986) *The Mathematical Modelling of Turbulent Flows*. Appl. Math. Models, vol. 10, pp. 190-220.